

## Phases in the $(1 - x)\text{Na}_{0.5}\text{Bi}_{0.5}\text{TiO}_3 - (x)\text{CaTiO}_3$ system

This article has been downloaded from IOPscience. Please scroll down to see the full text article.

2010 J. Phys.: Condens. Matter 22 075901

(<http://iopscience.iop.org/0953-8984/22/7/075901>)

View [the table of contents for this issue](#), or go to the [journal homepage](#) for more

Download details:

IP Address: 129.252.86.83

The article was downloaded on 30/05/2010 at 07:11

Please note that [terms and conditions apply](#).

# Phases in the $(1 - x)\text{Na}_{0.5}\text{Bi}_{0.5}\text{TiO}_3 - (x)\text{CaTiO}_3$ system

Rajeev Ranjan<sup>1</sup>, Rohini Garg<sup>1</sup>, V Kothai<sup>1</sup>, Anupriya Agrawal<sup>2</sup>, Anatoliy Senyshyn<sup>3</sup> and Hans Boysen<sup>4</sup>

<sup>1</sup> Department of Materials Engineering, Indian Institute of Science, Bangalore 560012, India

<sup>2</sup> Department of Materials Science and Engineering, Ohio State University, Columbus, OH 43210, USA

<sup>3</sup> Institute for Materials Science, Darmstadt University of Technology, Petersenstrasse 23, D-64287 Darmstadt, Germany

<sup>4</sup> Department für Geo- und Umweltwissenschaften, Sektion Kristallographie, Ludwig Maximilians Universität, Am Coulombwall 1, D-85748 Garching, München, Germany

E-mail: [rajeev@materials.iisc.ernet.in](mailto:rajeev@materials.iisc.ernet.in)

Received 6 August 2009, in final form 25 December 2009

Published 29 January 2010

Online at [stacks.iop.org/JPhysCM/22/075901](http://stacks.iop.org/JPhysCM/22/075901)

## Abstract

The structures of  $(1 - x)\text{Na}_{0.5}\text{Bi}_{0.5}\text{TiO}_3 - (x)\text{CaTiO}_3$  at room temperature have been investigated using neutron powder diffraction and dielectric studies. The system exhibits an orthorhombic ( $Pbnm$ ) structure for  $x \geq 0.15$  and rhombohedral ( $R3c$ ) for  $x \leq 0.05$ . For  $x = 0.10$ , though the neutron diffraction pattern shows features of the orthorhombic ( $Pbnm$ ) structure, Rietveld refinement using this structure shows a drastic reduction in the in-phase tilt angle ( $\sim 4^\circ$ ) as compared to the corresponding value ( $\sim 8^\circ$ ) for a neighbouring composition  $x = 0.15$ . The neutron diffraction pattern of  $x = 0.10$  could be fitted equally well using a two-phase model ( $R3c + Pbnm$ ) with orthorhombic as the minor phase (22%), without the need for a drastic decrease in the in-phase tilt angle. The dielectric studies of  $x = 0.10$  revealed the presence of the polar  $R3c$  phase, thereby favouring the phase coexistence model, instead of a single-phase  $Pbnm$  structure, for this composition.

(Some figures in this article are in colour only in the electronic version)

## 1. Introduction

The ferroelectric compound  $\text{Na}_{1/2}\text{Bi}_{1/2}\text{TiO}_3$  (NBT) has been extensively investigated for its dielectric and structural phase transition behaviour over the past four decades [1–5]. At room temperature NBT exhibits a polar rhombohedral structure (space group  $R3c$ ). The rhombohedral structure consists of a combination of an out-of-phase ( $a^-a^-a^-$  tilt system [6, 7]) tilt of adjacent oxygen octahedra about the threefold axis of the rhombohedral cell, and displacement of the cations and anions parallel to the polar axis. On heating above  $260^\circ\text{C}$ , the rhombohedral phase transforms to an intermediate tetragonal phase. The magnitude of the tetragonal strain is very small as compared to what is usually known for the classical ferroelectrics such as  $\text{BaTiO}_3$  and  $\text{PbTiO}_3$ . Based on analysis of the neutron powder diffraction pattern, the structure of this intermediate tetragonal phase has been reported to be different from the tetragonal structure of  $\text{BaTiO}_3/\text{PbTiO}_3$  [4]. The structure of the tetragonal phase of NBT consists of a

combination of in-phase ( $a^0a^0c^+$  tilt system) octahedral tilt about the fourfold axis, and cationic and anionic displacements along the polar axis [4]. The tetragonal and rhombohedral structures coexist over an extended temperature range [4]. The transition to the highest symmetry cubic structure occurs above  $540^\circ\text{C}$  [1–4]. The dielectric state of NBT in different temperature ranges has not been properly understood due to a lack of one-to-one correlation of the dielectric anomalies with the structural anomalies. NBT exhibits three anomalies in the temperature dependence of relative permittivity. The highest temperature anomaly occurs near 800 K [5]. The other two anomalies occur at  $\sim 640$  and  $\sim 540$  K and have been associated with the onset of an ‘antiferroelectric state’ [5] and ferroelectric states, respectively.

More recently, electron diffraction studies of the structures of NBT above room temperature have shown that the rhombohedral phase of NBT transforms into a modulated structure [8, 9]. This modulated structure has been explained

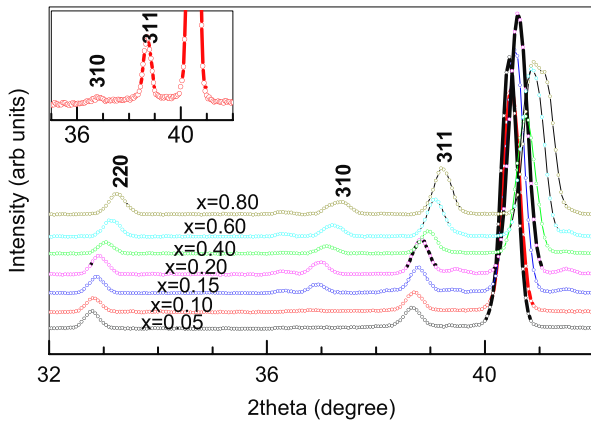


**Figure 1.** Neutron powder diffraction patterns of  $(1-x)\text{Na}_{0.5}\text{Bi}_{0.5}\text{TiO}_3-(x)\text{CaTiO}_3$  in a limited  $2\theta$  range. The indices are with respect to a doubled pseudocubic perovskite cell. The inset shows a magnified plot of  $x = 0.10$ .

in terms of the growth of orthorhombic sheets in rhombohedral blocks by a microtwinning process [8, 9]. The orthorhombic phase (space group  $Pbnm$ ) is formed at  $300^\circ\text{C}$  which immediately transforms into the tetragonal ( $P4bm$ ) phase reported earlier [4]. This study clearly suggests that the precursor phase of the rhombohedral structure is orthorhombic and not tetragonal, as has been considered so far. This new result calls for a fresh look into the correlation between the structure and dielectric behaviour of NBT. NBT is also considered as one of the important parent compounds for the development of lead-free piezoelectric materials [10, 11]. Many different solid solutions, such as with  $\text{BaTiO}_3$  [12, 13],  $\text{PbTiO}_3$  [14–17],  $\text{SrTiO}_3$  [18, 19],  $\text{KNbO}_3$  [20, 21] and  $\text{NaNbO}_3$  [21], have been investigated in this regard. A preliminary investigation of Ca-modified NBT has been reported recently [22]. In this paper, we report a detailed structural analysis of the Ca-modified NBT system using a neutron powder diffraction study. The orthorhombic phase of the  $\text{CaTiO}_3$  type is stabilized for  $x \geq 0.10$ , indicating that the rhombohedral phase of NBT is susceptible to orthorhombic distortion brought about by Ca substitution.

## 2. Experimental details

$(1-x)\text{NBT}-(x)\text{CT}$  samples were prepared using the conventional ceramic synthesis method. Stoichiometric amounts of  $\text{Na}_2\text{CO}_3$ ,  $\text{Bi}_2\text{O}_3$ ,  $\text{CaCO}_3$  and  $\text{TiO}_2$  (of purity greater than 99.5%) were thoroughly mixed for 6 h in zirconia jars containing zirconia balls and acetone as a mixing media, in a planetary ball mill. The mixed powders were calcined at  $900^\circ\text{C}$  for 3 h. The calcined powders were cold compacted and sintered in a temperature range  $1100\text{--}1250^\circ\text{C}$  (higher sintering temperature for higher calcium concentration). For diffraction studies, the sintered pellets were manually crushed with an agate mortar and pestle and annealed at  $700^\circ\text{C}$  for about 10 h to release the possible strain induced during the mechanical crushing. Neutron powder diffraction data at room temperature was collected at the SPODI powder diffractometer at FRM II, Germany, using a wavelength of  $1.548 \text{ \AA}$ . Structural analyses was carried out with the software ‘FULLPROF’ [23].

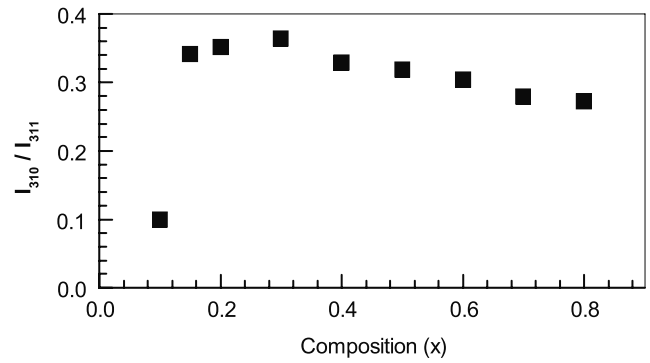


**Figure 2.** Variation of the ratio of the peak intensity of the doubled pseudocubic reflections 310 and 311 with composition.

For dielectric measurements, surfaces of the sintered pellets were gently polished, cleaned and painted with silver paste. The paste was cured at  $500^\circ\text{C}$  for 15 min. Capacitance and loss tangents were measured on selected compositions using a Novocontrol impedance analyser (Alpha AN) in the temperature range  $30\text{--}400^\circ\text{C}$ .

## 3. Results and discussion

### 3.1. Analysis of the neutron powder diffraction patterns

Figure 1 shows part of the neutron diffraction patterns of  $(1-x)\text{NBT}-(x)\text{CT}$  in a limited  $2\theta$  region. A visual inspection shows Bragg peaks of similar types for  $0.15 \leq x \leq 0.80$ . The indices in this figure are based on a doubled pseudocubic cell  $2a_p \times 2b_p \times 2c_p$ . As such, reflections with at least one odd index are the superlattice reflections [6, 7]. Following Glazer’s scheme, the superlattice reflections with all-odd and two-odd–one-even type indices are representative of out-of-phase (–) and in-phase (+) octahedral tilts, respectively [6, 7], in the structure. The 311 superlattice peak, corresponding to the out-of-phase tilt, is clearly observable for all the compositions. On the other hand, the 310 superlattice peak, corresponding to the in-phase octahedral tilt, could be seen clearly only for  $x \geq 0.15$ . A careful examination of the pattern of  $x = 0.10$ , however, revealed its presence for this composition as well (see the inset of figure 1) For  $x = 0.05$ , the two-odd–one-even type superlattice reflections are not visible, suggesting the absence of the in-phase tilt for  $x \leq 0.05$ . A plot of the ratio of the peak values of 311 and 310 reflections as a function of composition reveals an anomalous decrease at  $x = 0.10$  (see figure 2). It may be remarked that the intensities of the all-odd and odd–odd–even type reflections are a measure of the out-of-phase and in-phase tilt angles, respectively [6, 7]. In this context, the sharp drop of the intensity ratio ( $I_{310}/I_{311}$ ) below  $x = 0.15$  may be interpreted as the setting in of a criticality in the system, and hence an impending phase transition. This would imply that the orthorhombic ( $Pbnm$ ) structure is likely to transform to another structure, without an in-phase tilt component, somewhere between  $x = 0.10$  and  $0.05$ . Alternatively, it is also possible to explain the drastic decrease in the intensity of the 310, as compared to that of the 311, peak as a manifestation of the phase coexistence of the  $R3c$  phase (which would show only all-odd type peaks in

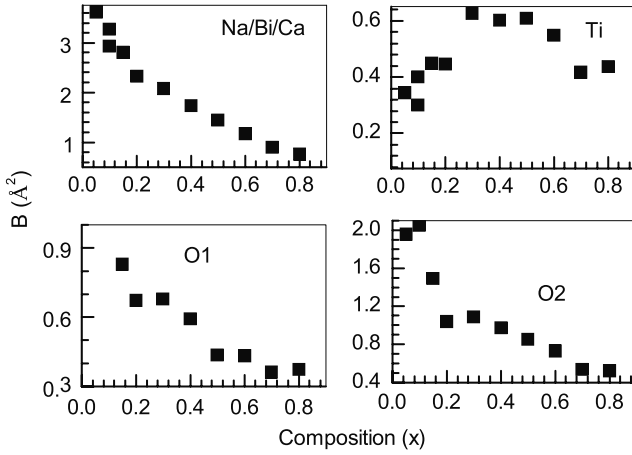


**Figure 3.** Composition variation of the isotropic displacement parameters ( $B$ ) of the atoms.

the pattern) and  $Pbnm$  phase (which would show both all-odd and two-odd–one-even type peaks) with a significantly reduced phase fraction of the latter phase. Rietveld analysis was carried out to check the plausibility of both models.

**3.1.1. Rietveld refinement.** As discussed above, since the diffraction patterns of the compositions  $0.10 \leq x \leq 0.80$  are consistent with the orthorhombic ( $Pbnm$ ) structure, Rietveld refinements of these compositions were accordingly carried out with this structural model. The asymmetric unit of this structure consists of one Na/Bi/Ca at  $(0 + \Delta x_{\text{Na/Bi/Ca}}, 0.5 + \Delta y_{\text{Na/Bi/Ca}}, 0.25)$ , one Ti at  $(0, 0, 0)$ , one oxygen (O1) at  $(0 + \Delta x_{\text{O1}}, 0 + \Delta y_{\text{O1}}, 0.25)$  and another oxygen (O2) at  $(0.25 + \Delta x_{\text{O2}}, 0.25 + \Delta y_{\text{O2}}, 0 + \Delta z_{\text{O2}})$ . The composition  $x = 0.05$  was refined with the rhombohedral ( $R3c$ ) structure. The asymmetric unit of the rhombohedral structure consists of one Na/Bi/Ca at  $(0, 0, 0.25 + \Delta z_{\text{Na/Bi/Ca}})$ , one Ti at  $(0, 0, 0 + \Delta z_{\text{Ti}})$  and one O occupying a site at  $(0.5 + \Delta x_{\text{O}}, 0 + \Delta y_{\text{O}}, 0.25 + \Delta z_{\text{O}})$ . In our refinement we have, however, followed the convention of Megaw and Darlington [24] in describing the various positional coordinates. This description allows for direct determination of the magnitude of the tilt angle ( $\omega$ ) about the pseudocubic [111] axis using the relationship  $\tan \omega = 4\sqrt{3}e$ , where  $e$  is determined from the refined values of the  $x$  and  $y$  coordinates of oxygen, described as  $(1/6 - 2e - 2d, 1/3 - 4d, 1/12)$ .

The isotropic atomic displacement parameter ( $B$ ) of the A-site cations was found to increase considerably as the composition approaches the NBT-rich end. The same trend was also observed for the  $B$  values of the O2 as shown in figure 3. Contrary to the  $B$  values of the A-site cations and oxygen, the  $B$  values of Ti are not affected significantly as a function of composition. The increase in the  $B$  values of the Na/Bi/Ca with increasing NBT fraction in the  $(1-x)\text{NBT}-(x)\text{CT}$  system suggests an increase in static disorder at the A site of the structure. One of the reasons for the large static disorder could be related to the presence of three different types of ions ( $\text{Na}^+$ ,  $\text{Bi}^{3+}$  and  $\text{Ca}^{2+}$ ) with slightly different ionic radii ( $r(\text{Na}^+) = 1.18 \text{ \AA}$ ,  $r(\text{Bi}^{3+}) = 1.17 \text{ \AA}$  and  $r(\text{Ca}^{2+}) = 1.12 \text{ \AA}$  [25]) occupying the A sites of the  $\text{ABO}_3$

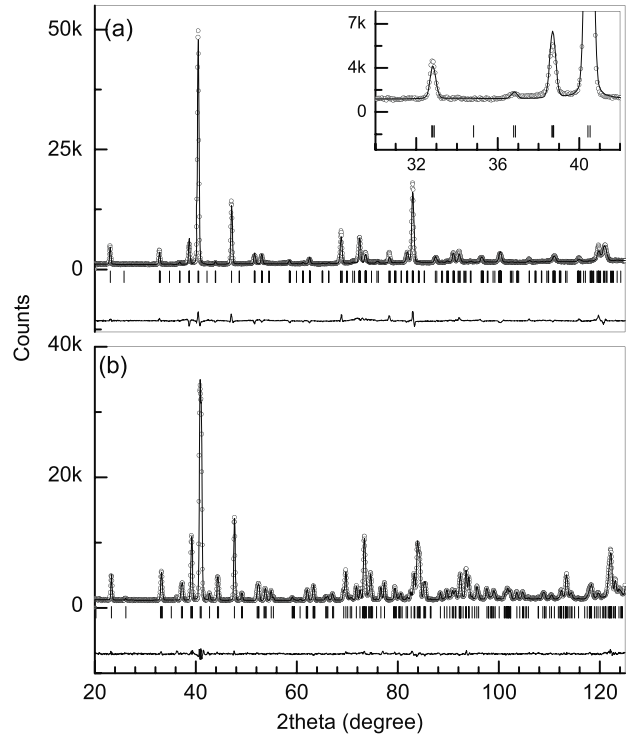


**Figure 4.** Rietveld plots of (a)  $x = 0.10$  and (b)  $x = 0.80$  after refinement with the orthorhombic ( $Pbnm$ ) structural model. The inset in (a) shows a magnified plot in a limited  $2\theta$  region to highlight the fitting of the weak superlattice reflections.

structure. In this context, the small value of the  $B(\text{Ti})$  and its relative insensitivity to the composition variation can be rationalized in terms of the absence of ionic disorder at the B site of this system. A slight improvement in the refinement was noted when the anisotropic atomic displacement parameters (ADPs) were varied for the atoms showing large  $B$  values. For the orthorhombic structures ADPs of Na/Bi/Ca and O2 were therefore refined. For  $x = 0.05$ , corresponding to the rhombohedral structure, ADP of Na/Bi/Ca and that of the only oxygen atom in the asymmetric unit was refined. For the rest of the atoms, isotropic displacement parameters ( $B$ ) were refined. Figure 4 shows Rietveld plots of two extreme compositions,  $x = 0.10$  and  $0.80$ , refined with the orthorhombic structure. Table 1 lists all the relevant structural parameters of the different compositions. In this table we have given the refined parameters of  $x = 0.10$  using the orthorhombic ( $Pbnm$ ) structural model. The Rietveld plot corresponding to  $x = 0.10$  suggests that the orthorhombic structural model can nicely account for the intensity anomaly.

The two out-of-phase ( $-$ ) tilts and the single in-phase ( $+$ ) tilt of the  $a^-a^-c^+$  tilt system of the orthorhombic ( $Pbnm$ ) structure was calculated using the coordinate of the O2 atom of the asymmetric unit. The equality of the two out-of-phase tilts about the two pseudocubic directions,  $[100]_p$  and  $[010]_p$ , can be described as a composite out-of-phase tilt about the  $[110]$  pseudocubic direction. The magnitude of the in-phase tilt ( $\psi$ ) about  $[001]_p$  and the out-of-phase tilt ( $\varphi$ ) about  $[110]_p$  were obtained from the displacements of the O2 atoms from  $(0.25, 0.25, 0)$  to  $(0.25 - u, 0.25 + v, w)$  using the expressions  $\tan \psi = 2(u + v)$  and  $\tan \varphi = 4\sqrt{2}w$ . The tilt angles

**Table 1.** Atomic coordinates, isotropic ( $B$ ) and anisotropic ( $\beta_{ij}$ ) displacement parameters of atoms for different compositions. The composition  $x = 0.05$  was refined with a rhombohedral ( $R3c$ ) structure. The rest were refined with an orthorhombic ( $Pbnm$ ) structure. The anisotropic displacement parameters are multiplied by  $10^4$ .

	$x = 0.05$	$x = 0.10$	$x = 0.15$	$x = 0.2$	$x = 0.3$	$x = 0.4$	$x = 0.5$	$x = 0.6$	$x = 0.7$	$x = 0.8$
$x(\text{Na/Bi})$	0	0.002(1)	0.004(1)	0.001(1)	0.000(1)	0.002(1)	0.004(1)	0.004(1)	0.004(1)	0.005(1)
$y(\text{Na/Bi})$	0	0.505(3)	0.516(1)	0.521(1)	0.521(1)	0.526(1)	0.529(1)	0.530(1)	0.532(1)	0.534(1)
$z(\text{Na/Bi})$	0.244(1)	0.25	0.25	0.25	0.25	0.25	0.25	0.25	0.25	0.25
$\beta_{11}(\text{Na/Bi})$	176(8)	154(33)	222(13)	156(9)	186(11)	142(11)	132(10)	118(9)	89(8)	66(7)
$\beta_{22}(\text{Na/Bi})$	176(8)	432(30)	398(19)	328(14)	265(14)	240(14)	191(12)	139(10)	110(8)	93(8)
$\beta_{33}(\text{Na/Bi})$	68(5)	137(23)	48(8)	52(5)	43(5)	33(7)	22(5)	20(5)	14(4)	19(4)
$\beta_{12}(\text{Na/Bi})$	-88(4)	60(24)	33(10)	30(7)	34(8)	18(9)	-2(8)	0(7)	8(6)	17(6)
$\beta_{13}(\text{Na/Bi})$	0	0	0	0	0	0	0	0	0	0
$\beta_{23}(\text{Na/Bi})$	0	0	0	0	0	0	0	0	0	0
$z(\text{Ti})$	-0.001(2)	0	0	0	0	0	0	0	0	0
$B(\text{Ti}) (\text{\AA}^2)$	0.81(6)	1.05(6)	0.87(5)	0.60(4)	0.70(4)	0.88(5)	0.85(5)	0.71(4)	0.56(4)	0.55(4)
$x(\text{O}_1)$		-0.050(1)	-0.056(5)	-0.059(4)	-0.062(1)	-0.064(1)	-0.067(1)	-0.068(1)	-0.068(1)	-0.069(1)
$y(\text{O}_1)$		-0.003(2)	-0.009(1)	-0.009(1)	-0.011(1)	-0.013(1)	-0.014(1)	-0.014(1)	-0.016(3)	-0.015(1)
$BO_1 (\text{\AA}^2)$		0.88(7)	1.02(5)	0.77(4)	0.74(4)	0.80(5)	0.56(4)	0.55(4)	0.45(3)	0.44(3)
$x(\text{O}_2)$	0.126(1)	0.231(1)	0.217(1)	0.216(1)	0.214(1)	0.213(1)	0.212(1)	0.212(1)	0.212(1)	0.211(1)
$y(\text{O}_2)$	0.338(2)	0.264(1)	0.280(4)	0.283(1)	0.285(1)	0.286(1)	0.287(1)	0.288(1)	0.289(1)	0.289(1)
$z(\text{O}_2)$	0.08333	0.026(1)	0.027(1)	0.028(1)	0.029(1)	0.032(1)	0.033(1)	0.034(1)	0.035(1)	0.036(1)
$\beta_{11}(\text{O}_2)$	345(32)	249(17)	137(7)	75(4)	98(5)	82(5)	56(4)	49(4)	38(4)	41(4)
$\beta_{22}(\text{O}_2)$	110(12)	399(20)	69(6)	55(4)	59(5)	58(5)	59(5)	53(4)	35(4)	37(4)
$\beta_{33}(\text{O}_2)$	47(3)	105(8)	75(4)	57(3)	52(3)	47(3)	46(3)	37(3)	29(2)	26(2)
$\beta_{12}(\text{O}_2)$	170(26)	-325(9)	-116(5)	-77(4)	-97(5)	-84(5)	-62(5)	-49(4)	-39(4)	-28(4)
$\beta_{13}(\text{O}_2)$	-63(9)	31(10)	-14(4)	17(3)	-16(3)	15(3)	17(3)	13(3)	9(2)	5(2)
$\beta_{23}(\text{O}_2)$	-45(3)	27(14)	-11(4)	-14(3)	-15(3)	-12(3)	2(3)	0(2)	-2(2)	-2(2)

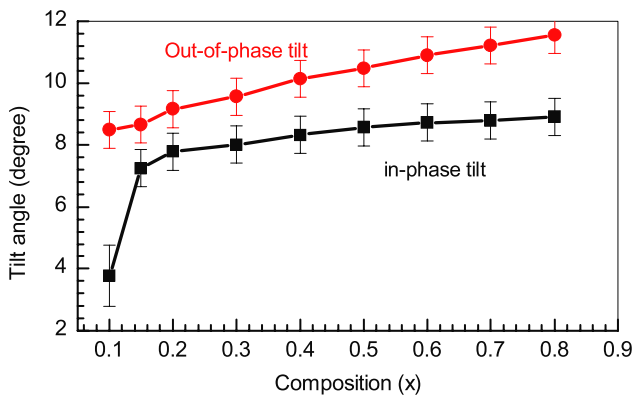


**Figure 5.** Variation of out-of-phase and in-phase tilt angles of the orthorhombic structures with composition.

obtained in this way is plotted in figure 5 as a function of composition. The out-of-phase tilt decreases from  $11.5^\circ$  to  $8.5^\circ$  when the value of  $x$  decreased from  $x = 0.8$  to  $0.10$ . The in-phase tilt angle decreases by a small amount (from  $9.0^\circ$  to  $7.2^\circ$ ) in the composition range  $0.15 \leq x \leq 0.80$ , and then drops suddenly to a value of  $3.8^\circ$  at  $x = 0.10$ . There can be two explanations to account for this situation: (i) the magnitude of the in-phase tilt is critically decreasing due to an incumbent phase transition from orthorhombic to another structure that has no in-phase (+) component of octahedral tilt, and (ii) the two phase ( $Pbnm + R3c$ ) model. There are six possible structures without any in-phase tilt component. They are consistent with the space groups (i)  $I4/mcm$  (tilt system  $a^0a^0c^-$ ), (ii)  $Imma$  (tilt system  $a^0b^-b^-$ ), (iii)  $R\bar{3}c$  (tilt system  $a^-a^-a^-$ ), (iv)  $C2/m$  (tilt system  $a^0b^-c^-$ ), (v)  $C2/c$  (tilt system  $a^-b^-b^-$ ) and (vi)  $P\bar{1}$  (tilt system  $a^-b^-c^-$ ) [26]. It has been commonly found that the orthorhombic ( $Pbnm$ )

structure transforms to cubic structures either by composition change or temperature via intermediate structures with space group  $Imma$  and/or  $I4/mcm$  [27–31]. In the present case, since the rhombohedral structure of the parent compound NBT is retained for  $x = 0.05$ , the drastic decrease in the in-phase tilt angle for the intermediate composition  $x = 0.10$  may not necessarily be indicative of an impending intermediate phase of the above type ( $Imma$  or  $I4/mcm$ ). Furthermore, since the two structures  $R3c$  and  $Pbnm$  of the neighbouring compositions,  $x = 0.05$  and  $0.15$ , respectively, are not group-subgroup-related, a transition from one structure to the other would necessarily be of a first-order nature. A coexistence of both phases is therefore a very likely possibility in the critical composition region. In view of this, a two-phase ( $R3c + Pbnm$ ) refinement was also performed for the composition  $x = 0.10$ . Because of the uncertainty in the beginning about the dominant phase contributing to the intensities of the various peaks in the neutron diffraction pattern, the coordinates of the atoms in the  $R3c$  and  $Pbnm$  phases were initially fixed at values corresponding to those obtained for  $x = 0.05$  and  $0.15$ , respectively. Further, to keep the number of refinable parameters at a minimum, only the isotropic displacement parameters of both phases were refined. During the final cycles of refinement, all the parameters were simultaneously varied without any constraint. The refinement with the two-phase model was found to be equally successful as with the single-phase  $Pbnm$  model, with a slightly improved goodness-of-fit for the two-phase model ( $\chi^2(Pbnm) = 1.62$ ;  $\chi^2(Pbnm + R3c) = 1.29$ ). For the sake of comparison of the  $R$  factor, refinement with the single-phase  $Pbnm$  model was also carried out with isotropic displacement parameters. Figure 6 shows the Rietveld plot corresponding to the two-phase model. The refined structural parameters obtained with the  $R3c + Pbnm$

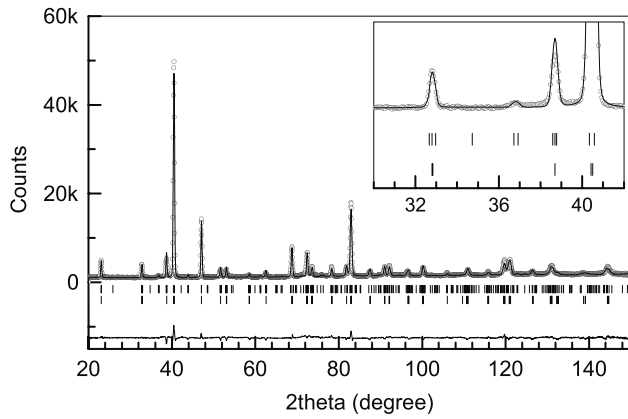


**Figure 6.** Rietveld plot for  $x = 0.10$  after refinement with the rhombohedral ( $R3c$ ) + orthorhombic phase ( $Pbnm$ ) coexistence model. The inset shows a magnified plot in a limited  $2\theta$  region to highlight the fitting of the superlattice reflections. The upper and lower vertical bars correspond to peak positions of the orthorhombic and rhombohedral phases, respectively.

model is listed in table 2. Both the in-phase and out-of-phase tilt angles of the orthorhombic phase, calculated from the refined oxygen (O2) coordinate, was found to be  $\sim 8(\pm 1)$ . This value is similar to the values obtained for the neighbouring composition  $x = 0.15$  (see figure 5). The result therefore shows a large discrepancy between the in-phase tilt angle calculated from the single-phase ( $Pbnm$ ) ( $\sim 4^\circ$ ) model and two-phase ( $Pbnm + R3c$ ) model ( $\sim 8^\circ$ ). In the two-phase refinement, the drastically reduced intensity of the 310 superlattice peak is taken care of by decreasing the fraction of the orthorhombic phase ( $22 \pm 1\%$ ), without the need to decrease the in-phase tilt angle drastically. Although  $\chi^2$  is slightly lower for the two-phase model (1.29) as compared to the single-phase orthorhombic model (1.62), this may not be given serious consideration since the number of refinable parameters in the two-phase model is more compared to the single-phase model. From the above analysis it is therefore clear that the ambiguity with regard to the phase of  $x = 0.10$  could not be resolved using neutron powder diffraction data.

### 3.2. Dielectric studies

Figure 7 shows the temperature dependence of the real and the imaginary part of the relative permittivity of  $x = 0.05, 0.10$  and  $0.15$  at different frequencies. For  $x = 0.05$ , the shape of the plot resembles very similar to the parent compound  $\text{Na}_{0.5}\text{Bi}_{0.5}\text{TiO}_3$  (NBT) [5, 17]. In analogy with NBT, the permittivity dispersion below  $250^\circ\text{C}$  can be attributed to the relaxor ferroelectric behaviour of the system. For NBT this feature occurs at  $\sim 225^\circ\text{C}$  and the ferroelectric state has been reported to survive until  $\sim 275^\circ\text{C}$  [5]. The nature of the broad anomaly above  $400^\circ\text{C}$  for  $x = 0.05$  also resembles that of NBT. The origin of this anomaly is still unclear in the literature. Similar to  $x = 0.05$ , the relative permittivity of  $x = 0.10$  shows a broad peak at  $\sim 175^\circ\text{C}$ . This suggests that the electrical (and corresponding structural) phase of  $x = 0.10$  at room temperature should be similar to that of  $x = 0.05$ . Since the orthorhombic structure considered above ( $Pbnm$ ) is centrosymmetric and hence is not anticipated to show a

**Table 2.** Structural parameters of the rhombohedral ( $R3c$ ) and orthorhombic ( $Pbnm$ ) phases for  $x = 0.10$  after two-phase refinement.

Phase: $R3c$	$x$	$y$	$z$	$B$ ( $\text{\AA}^2$ )
Na/Bi/Ca	0.0	0.0	0.249(1)	2.92(7)
Ti	0	0	0.015(1)	0.1(1)
O1	0.1242(8)	0.341(1)	0.0833	2.05(4)
Lattice parameters ( $\text{\AA}$ )	$a = 5.4767(2)$		$c = 13.442(1)$	
Phase: $Pbnm$				
Na/Bi/Ca	0.001(4)	0.496(5)	0.25	3.2(2)
Ti	0	0	0	0.3(2)
O1	-0.057(2)	0.002(3)	0.25	0.2(2)
O2	0.213(1)	0.287(1)	0.026(1)	1.4(2)
Lattice parameters ( $\text{\AA}$ )	$a = 5.4591(9), b = 5.5055(8) c = 7.755(2)$			
R-factors	$R_p = 5.81, R_{wp} = 7.61, R_e = 6.69, \chi^2 = 1.29$			
Percentage phase fraction	$R3c = 78 \pm 1\%, Pbnm = 22 \pm 1\%$			

dielectric anomaly above room temperature, the dielectric anomalies of  $x = 0.10$  are attributed to the rhombohedral ( $R3c$ ) phase. Hence, in view of the arguments presented in section 3.1.1, the dielectric result is consistent only with the phase coexistence model and not with the single-phase orthorhombic ( $Pbnm$ ) model.

Contrary to  $x = 0.05$ , the permittivity of  $x = 0.15$  does not show a peak above room temperature. There is, however, a tendency for saturation of the permittivity near room temperature, suggesting a possibility of a permittivity maximum at a temperature close to room temperature. In view of this, a possibility of occurrence of the rhombohedral phase below room temperature cannot be ruled out. To determine if a fraction of this phase exists even at room temperature, the neutron data of  $x = 0.15$  was revisited using the phase coexistence ( $Pbnm + R3c$ ) model. The fraction of the rhombohedral and the orthorhombic phases was, however, found to be 2% and 98%, respectively. This ruled out any significant presence of the rhombohedral phase at room temperature for  $x = 0.15$ , and confirmed the validity of the refinement with a single-phase orthorhombic ( $Pbnm$ ) model for  $x = 0.15$ , reported in section 3.1.1.

## 4. Conclusions

The system  $(1-x)\text{Na}_{0.5}\text{Bi}_{0.5}\text{TiO}_3-(x)\text{CaTiO}_3$  shows miscibility in the entire composition range. The Bragg reflections in the neutron powder diffraction patterns of the compositions  $0.10 \leq x \leq 0.80$  appear similar, thereby suggesting similarity of the structure. However, the intensity of the Bragg peaks corresponding to odd-odd-even indices (indexed on a doubled pseudocubic axes) decrease very abruptly for the composition  $x = 0.10$ . This feature could be explained in two different ways: (i) by considering an abrupt decrease in the in-phase tilt angle of the oxygen octahedra of the orthorhombic ( $Pbnm$ ) structure and (ii) in terms of coexistence of the orthorhombic ( $Pbnm$ ) and rhombohedral ( $R3c$ ) structures for

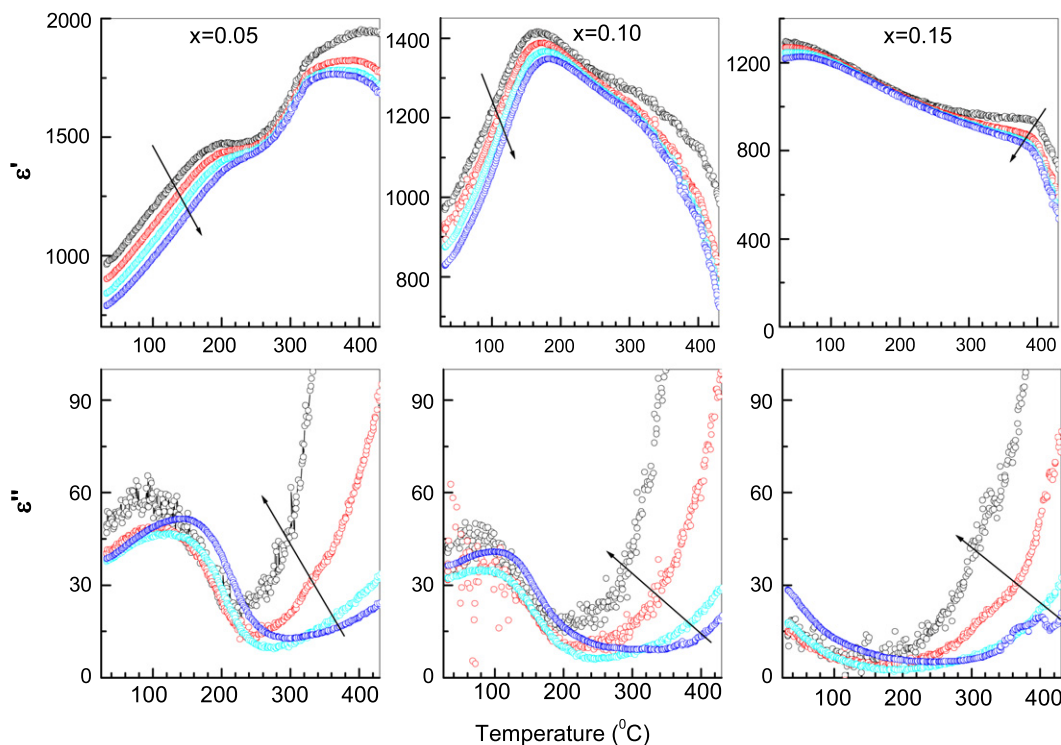


**Figure 7.** Temperature dependence of the real ( $\epsilon'$ ) and imaginary ( $\epsilon''$ ) parts of  $(1-x)\text{Na}_{0.5}\text{Bi}_{0.5}\text{TiO}_3-(x)\text{CaTiO}_3$  at 1, 10, 100 kHz and 1 MHz. The arrows indicate the data points corresponding to increasing frequency.

the composition. In the latter case, the in-phase tilt angle did not exhibit any anomalous decrease. Instead, the anomalous decrease in the intensity of the odd–odd–even type reflections could be accounted for in terms of the reduced fraction of the orthorhombic ( $Pbnm$ ) phase (22%) as compared to the rhombohedral phase (78%). Temperature-dependent dielectric studies of  $x = 0.10$  showed features which, to a significant extent, resemble the rhombohedral composition rather than the neighbouring orthorhombic composition. This helped in settling the correct model as  $Pbnm + R3c$  for  $x = 0.10$ . It may be remarked that the stabilization of a  $\text{CaTiO}_3$ -type orthorhombic ( $Pbnm$ ) phase in this system for Ca concentration as low as  $x = 0.10$  may be related to the intrinsic instability of NBT with regard to such an orthorhombic ( $Pbnm$ ) distortion, as has been reported recently [8, 9].

## References

- [1] Vakhrushev S B, Ivanitskii B G, Kvyatkovskii B E, Maisternko A N, Malysheva R S, Okuneva N M and Parfenova N N 1983 *Fiz. Tverd. Tela* **25** 2613
- [2] Vakhrushev S B, Ivanitskii B G, Kvyatkovskii B E, Maisternko A N, Malysheva R S, Okuneva N M and Parfenova N N 1983 *Sov. Phys.—Solid State* **25** 1504 (Engl. Transl.)
- [3] Suchanicz J and Kwapulinski J 1995 *Ferroelectrics* **195** 249
- [4] Jones G O and Thomas P A 2002 *Acta Crystallogr. B* **58** 168
- [5] Jones G O and Thomas P A 2000 *Acta Crystallogr. B* **56** 426
- [6] Tu C S, Siny I G and Schmidt V H 1994 *Phys. Rev. B* **49** 11550
- [7] Glazer A M 1972 *Acta Crystallogr. B* **28** 3384
- [8] Glazer A M 1975 *Acta Crystallogr. A* **31** 756
- [9] Dorcet V, Trolliard G and Boullay P 2008 *Chem. Mater.* **20** 5061
- [10] Trolliard G and Dorcet V 2008 *Chem. Mater.* **20** 5074
- [11] Takenaka T, Maruyama K and Sakata K 1991 *Japan. J. Appl. Phys.* **30** 2236
- [12] Takenaka T, Nagata H, Hirma Y, Yoshii Y and Matumoto K 2007 *J. Electroceram.* **19** 259
- [13] Chiang Y M, Farrey G W and Soukhojak A N 1998 *Appl. Phys. Lett.* **73** 3683
- [14] Hosono Y, Harada K and Yamashita Y 2001 *Japan. J. Appl. Phys.* **40** 5722
- [15] Elkechai O, Marchel P, Thomas P, Manier M and Mercurio J P 1997 *J. Mater. Chem.* **7** 91
- [16] Sakata K, Takenaka T and Naitou Y 1992 *Ferroelectrics* **131** 219
- [17] Park S E and Hong K S 1996 *J. Appl. Phys.* **79** 383
- [18] Hong K S and Park S E 1996 *J. Appl. Phys.* **79** 388
- [19] Sakata K and Masuda Y 1974 *Ferroelectrics* **7** 347
- [20] Park S E and Hong K S 1997 *J. Mater. Res.* **12** 2152
- [21] Ishii H, Nagata H and Takenaka T 2001 *Japan. J. Appl. Phys.* **40** 5660
- [22] Wada T, Toyoiike K, Imanaka Y and Matsuo Y 2001 *Japan. J. Appl. Phys.* **40** 5703
- [23] Ranjan R, Kothai V, Garg R, Agrawal A, Senyshyn A and Hoysen H 2009 *Appl. Phys. Lett.* **95** 042904
- [24] Rodrigues-Carvajal J 2000 *FULLPROF. A Rietveld Refinement and Pattern Matching Analysis Program* Laboratoire Leon Brillouin (CEA-CNRS) France
- [25] Megaw H D and Darlington C N W 1975 *Acta Crystallogr. A* **31** 161
- [26] Shannon R D 1976 *Acta Crystallogr. A* **32** 751
- [27] Howard C J and Stokes H T 2005 *Acta Crystallogr. A* **61** 9
- [28] Howard C J, Knight K S, Kennedy B J and Kisi E H 2000 *J. Phys.: Condens. Matter* **12** L677
- [29] Kennedy B J, Hunter B A and Hester J R 2002 *Phys. Rev. B* **65** 224103
- [30] Mountstevens E H, Attfield J P and Redfern S A T 2003 *J. Phys.: Condens. Matter* **15** 8315
- [31] Li L, Kennedy B J, Kubota Y, Kato K and Garrett R F 2004 *J. Mater. Chem.* **14** 263
- [32] Ranjan R, Agrawal A, Senyshyn A and Boysen H 2006 *J. Phys.: Condens. Matter* **18** 9679